ARCHIVES
of
FOUNDRY ENGINEERING

ISSN (2299-2944)

10.24425/afe.2024.151286

Published quarterly as the organ of the Foundry Commission of the Polish Academy of Sciences

Research of Hybrid Aluminium Castings with the Use of Porous Cores

M. Brůna [a], M. Medňanský [a, *], P. Oslanec [b]

[a] Faculty of Mechanical Engineering, Department of Technological Engineering, University of Zilina, Univerzitná 8215/1, 010 26 Žilina, Slovak Republic

[b] Institute of Materials and Machine Mechanics, Slovak Academy of Sciences, Inoval - Innovation center, Priemyselná 525 Ladomerská Vieska, 965 01 Žiar nad Hronom, Slovak Republic

* Corresponding author: E-mail address: martin.mednansky@fstroj.uniza.sk

Received 23.04.2024; accepted in revised form 10.06.2024; available online 22.07.2024

Abstract

The paper focuses on the research of hybrid aluminium castings produced by overcasting technology. This is an advanced technology for ensuring the lightness of castings by using the principle of overcasting a core with a porous cellular structure produced by foaming. Process parameters in the foaming phase of the material have a great influence on the resulting porous structure. The article focuses on controlling the influence of pressure during the foaming process on the resulting porosity and evaluating by X-ray tomograph and measuring the relative density. Variants using an initial pressure of 0.3 MPa appear to be the most satisfactory. The challenge of this technology is to ensure adequate bonding of the metals at the interface between the porous core and the solidified metal without penetrating the coating layer. For this reason, the surface treatment of foamed cores with various etchants has been proposed to disrupt the oxide layer on their surface. Macrographs of the uncoated sample and samples etched with 0.5% HF and 10% H_3PO_4 demonstrated the need for core surface treatment to prevent liquid metal penetration. EDX analysis confirmed the presence of $AlPO_4$ at the core/casting interface in the treated sample.

Keywords: Hybrid castings, Aluminium foams, Porous materials, Lightweighting

1. Introduction

In an effort to achieve carbon neutrality, the automotive industry is using a variety of technologies to reduce the weight of its products. The goal is to save energy and reduce emissions. Nearly 60% of aluminium automotive components are produced by high pressure die casting. Despite efforts to use secondary alloys in the die casting process, it is still energy-intensive and has a significant environmental impact [1-3]. The second modern approach to weight reduction is topological optimization of the structure. This results in a complex shape of the part, which often cannot be produced by conventional casting technologies [4,5]. Usually, the production is carried out by additive technologies, which are currently still unprofitable for mass production.

The proposed alternative approach in this paper is the overcasting technology. It is one of the technologies for joining (chemically similar, but also different) metals, where solid and liquid materials are joined. Compared with other metal joining methods (soldering, explosive welding, hydrostatic extrusion, continuous casting, etc.), it is considered to be the best joining technique due to its superior characteristics, including high production efficiency, performance, design flexibility, weight saving, and low operating cost (comapred to high pressure die casting for example) [6].

Overcasting is defined as a manufacturing technology in which two metals, one in the solid state and the other in the liquid state, are brought into contact with each other so that a diffusion reaction zone is formed between the two materials, resulting in a smooth transition from one metal to the other [7]. Due to the above

mentioned advantages, overcasting technology has recently received a lot of attention in various design solutions.

To ensure weight reduction of hybrid aluminium castings produced by overcasting technology, it is proposed to use aluminium foam as a solid medium. It is a porous material that is characterized by low weight, thermal and acoustic insulation, and energy absorption [8].

The properties of metal foam depend on the type of porosity (open/closed), which is determined by the technology of its production. The foaming temperature influences the pore size and the resulting porosity. A low temperature does not allow the material to expand to the required level, while a high temperature causes the pores to collapse and gas to escape from the structure. The ambient atmosphere affects the foaming process if the alloy contains additives with a high affinity for oxygen. The time of foaming affects the surface oxidation - during slow foaming the presence of oxides increases. [9] This paper focuses on the influence of the pressure acting during foaming on the resulting relative density and the possibility of its control.

The main challenge of this process is the bonding of materials during the casting of metal foam with molten metal of similar chemical composition, because on the surface of the solid core, as well as on the surface of the melt encapsulating the porous core, oxide layers of Al_2O_3 with a melting temperature of 2072 °C, which fundamentally limits the wettability of the aluminium core [10]. One of the solutions is the chemical replacement of the Al_2O_3 surface with a zinc layer (lower melting temperature: 420 °C) [7]. However, in this paper a simpler principle of chemical disruption of the oxide layer is used, by etching the surface.

This work presents a methodology of realisation and testing of this novelty composite. Due to the advantageous properties of foam cores, the hybrid castings might find their use in the automotive industry as chassis elements that dampen vibrations generated by the engine or as shaped crash boxes. In the aerospace industry, hybrid designs may be of interest to reduce the weight of drones, thereby providing greater range distance.

2. Methodology and materials

In the experimental work the technology of foaming of hot pressed metal powder was used for production of the cores, i.e. production of metal foam by means of powder metallurgy. Its principle is to heat an isostatic mixture of aluminium alloy powders and TiH_2 foaming agent to a temperature close to the melting point of the base alloy. Under the effect of temperature and pressure, hydrogen gas is released. The developed pressure expands the semi-finished product into a highly porous structure with closed pores. [11]

The basis of the powder mixture used was Al99.5 powder (with an average fraction < 400 μm) with the addition of 10 wt% Si powder (< 20 μm) and 0.8 wt% foaming agent TiH_2 powder (< 5 μm).

In the first step, samples in the form of a plate with dimensions of 15 x 55 x 55 mm were foamed in order to first determine the influence of the applied pressure when foaming cores with simple geometry. The foaming temperature was 680 °C. The pressure of the atmosphere (N_2) in the foaming chamber changed rapidly from the initial pressure to the stabilization pressure, which acts as a counterpressure against the bubbles of released hydrogen. The variants of foaming pressures during the realization of individual samples are shown in Table 1. Eight samples were foamed, while three different stabilization pressures were used for sub-variants A2 and A3. The time course of temperature and pressure during foaming is shown in Fig.1.

Table 1.
Foaming pressure variants for preliminary plate samples

Variant	Starting pressure [MPa]	Stabilising pressure [MPa]
A0	Atmospheric	Atm.
A1	0.1	Atm.
A2a/b/c	0.2	Atm. / 0.05 / 0.1
A3a/b/c	0.3	0.1 / 0.15 / 0.2

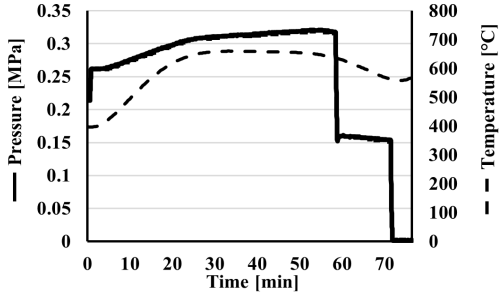

Fig. 1. Foaming process (A3b variant)

The porosity was analyzed using a Nikon XT H225 ST computer tomograph - the average Feret's pore diameter and its standard deviation were determined. The results of this stage of the experiment were decisive for the further selection of parameters in the next stage of the research.

Foamed cores intended for overcasting are more complex, cylindrical shapes, with geometry of which is shown schematically in Figure 2. The protrusions on the sides of the cylinder serve to position the core in the mold cavity and also to mechanically bond the core to the future casting.

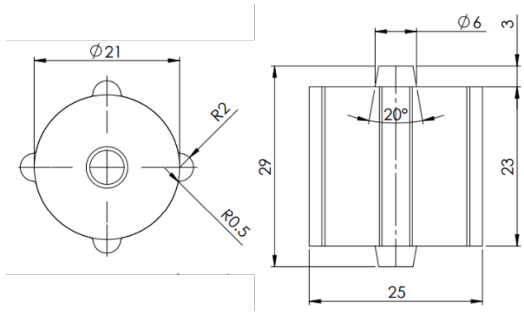

Fig. 2. Dimensions of the foamed core

A reusable three-part permanent mold was designed and milled from 99.9% graphite ingot block, with 28 cavities (Fig. 3a). During the foaming process, a nitrogen gas atmosphere is used in the foaming chamber (Fig. 3b) to prevent the degradation of the graphite form by oxidation at elevated temperature. The foaming temperature was 680 °C.

a) b)

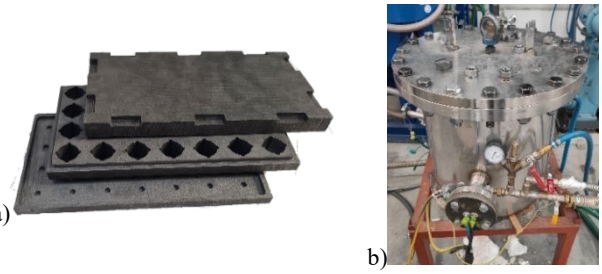

Fig. 3. Core foaming tools: a) Graphite block foaming die; b) Foaming chamber

Cores were foamed at different initial and stabilization pressures according to Table 2.

Table 2.
Foaming pressure variants for the batches of cylindrical cores

Variant	Starting pressure [MPa]	Stabilising pressure [MPa]
B1	Atmospheric	0.005 ± 0.002
B2	0.15 – 0.2	0.15.
B3/B4/B5/B6	0.1 – 0.2	0.1 / 0.15 / 0 .05 / Atm.
B7	0.1 – 0.3	0.15

In the case of foamed cores, the weight of five samples from each B variant was measured using a laboratory scale to express the relative density ρ/ρ_S according to relation (3) based on the relations (1) and (2):

$$\rho_S = m_S / V \quad (1)$$

$$\rho = m / V \quad (2)$$

$$\rho / \rho_S = m / m_S \quad (3)$$

where m and ρ are the weight and density of the foamed component [g, respectively. g.mm^{-3}], m_S [g] is the mass of the solid component with the same volume V [mm^{-3}] as the foamed component, and ρ_S is the density of the base material.

Selected variants of foamed cores intended for overcastin were surface treated according to Table 3.

Table 3.
Variants of the surface treatment

	N	F	P1	P4
1	Degreasing by rubbing each side with isopropylalcohol			
2	Drying (all 4 variants)			
3	x	Bathing each side in HF 0.5% for 20 s	Bathing each side in H_3PO_4 10% for 1:30 min at 50 °C	Bathing each side in H_3PO_4 10% for 4:00 min at 50 °C
4	x	Drying	Drying	Drying
5	x	Rubbing each side with 99.5% isopropylalcohol		
4	x	Drying	Drying	Drying
6	Preheating in electric resistance furnace at 150 ± 10 °C for 15 minutes			

The molds used for casting were made from second generation sand blocks using a patternless process because of their high repeatability, good breathability, and disintegration after casting. The self-hardening mixture was prepared by mixing sand fractions 34 (0.1-0.4 mm) and 33 (0.1-0.5 mm) in a ratio of 4:3 with phenol-formaldehyde resin and then cured by CO_2. The dimensions of the blocks were 300x145x50 mm. Next, the gating system and three cavities in each half mold were CNC milled and graphite coating was applied to the surface of the gating system, mold cavities, and vertical parting plane to reduce mold brittleness and support fluidity. The preheated cores were placed in the mold cavity and the mold was preheated at a temperature of 150 ± 10 °C for 15 minutes.

AlSi7Mg0.3 alloy was selected for overcasting foamed cores by using standard gravity casting technology. The alloy was selected because it is suitable for casting in sand molds, permanent molds, and also shell molds. The choice of this alloy was also conditioned by the perspective of ongoing research into the effect of heat treatment on the mechanical properties of castings. Chemical composition of used alloy is shown in Table 4. The material was melted in an electric resistance furnace at a casting temperature of 760 ± 10 °C.

Table 4.
Chemical composition of the AlSi7Mg0.3 alloy [wt%]

Si	Mg	Fe	Mn	Ti
6.5 – 7.5	0.25 – 0.45	max. 0.19	max. 0.1	max. 0.25
Cu	**Zn**	**Others**		**Al**
max. 0.05	max. 0.07	each 0.03; total 0.1		balanced

Macroscopic observation of the selected hybrid castings was performed using an Olympus SZX16 stereomicroscope, and microscopic observation/EDX analysis of selected samples were performed using a TESCAN LMU II scanning electron microscope with a Bruker EDX analyzer.

3. Results and Discussion

3.1. Porosity analysis

The number and dimensions of pores in the cross-section of the samples were analyzed using the ImageJ program (Fig. 4). The maximum Feret's diameter, mean Feret's diameter and standard deviation were plotted (Fig. 5).

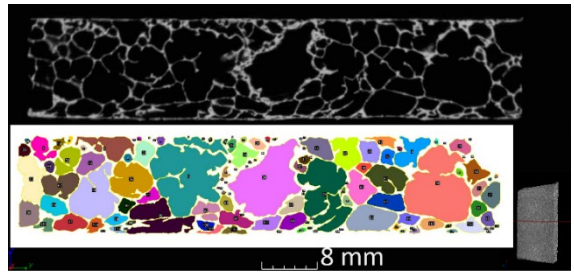

Fig. 4. Pore amount in the cross-section of A3a sample, computer tommography

The largest difference between maximum and mean Feret's pore diameter was observed in all three sub-variants of A2. The largest Feret's pore diameter (13,923 mm) and the largest standard deviation (1,728 mm) were measured in variant A2b. The largest average Feret's pore diameter was recorded in variant A2c (1,331 mm). Due to the increased number of large pores per constant volume, all A2 sub-variants had reduced pore numbers compared to the other variants. It can be concluded that the initial pressure of 0.2 MPa has no positive effect on the porosity character.

Samples foamed with initial pressure A3 (0.3 MPa) showed a larger number of pores (the maximum number of pores was recorded in sample A3a, 316 pores) and generally lower values of the maximum and average Feret's pore diameter. Among the A3 sub-variants, the smallest mean and maximum Feret's pore diameters were recorded in the A3a variant.

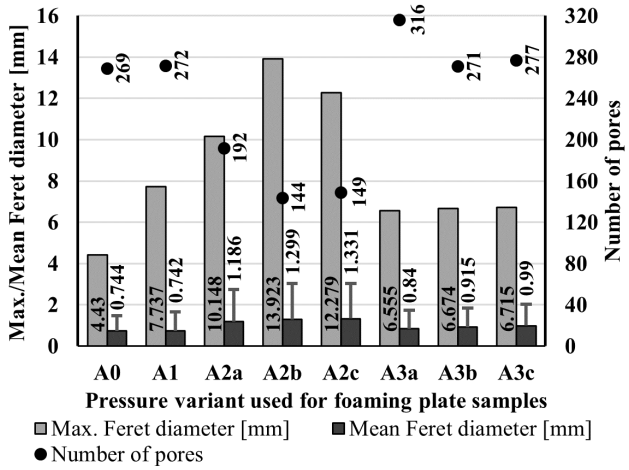

Fig. 5. Number and Feret's diameter of pores in evaluated plate samples

Based on these results, three variants of foamed cores were selected for overcasting. B1 as a reference sample foamed at atmospheric pressure, then B7 as a sample foamed under conditions the most similar to plate sample A3a (0.1 - 0.3 / 0.15 MPa), and sample B5, which will serve as a control sample when using foaming pressures at approximately halved values (0.1 - 0.2 / 0.05 MPa).

3.2. Relative density of the foamed cores

The weight of five samples of all seven core variants was measured. The measured values and the mass of the solid body determined from the properties of the CAD model were used to calculate the relative density using equation (3). The mean values of the results for each variant and their standard deviation are shown graphically in Figure 6.

The lowest mean value of relative density (and therefore the highest value of porosity) was measured on variant B2 (± 18.3%), but the measurements on this variant had the highest standard deviation (± 3.6%). The lowest standard deviation, which results in the lowest variability of results within a variant, was found on variant B6 (± 0.8%). Low variability was also found for variant B7 (± 1.6%). The highest mean value of relative density was found in samples of variety B3 (21.5%), but again this result was accompanied by a high standard deviation (± 3.6%).

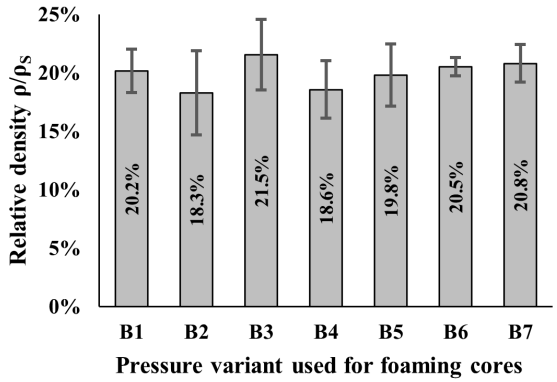

Fig. 6. Relative density dependance on the foaming pressures

Visual inspection revealed that the coating layer of some foamed cores was not uniform, but the wall was disturbed. Due to this fact, an increased effort was made to select samples whose surface was not disturbed.

Selected foamed cores (B1, B5, B7) were surface modified by etching according to Table 3 (Figure 7). On cores treated with H_3PO_4, a color change of the core surface to a matte silver color was observed. It is believed that an acid-base neutralization reaction occurred on the surface:

$$Al_2O_3 + 2\ H_3PO_4 \rightarrow 2\ AlPO_4 + 3\ H_2O \quad (4)$$

The product of such a reaction is aluminium phosphate, the light color of which indicates its presence on the surface of the core as shown in Figure 7c. Surface treatment with hydrofluoric acid did not result in a fundamental change in surface color.

a) b) c)

Fig. 7. Foamed cores with varying surface treatments: a) non-etched, b) etched with HF, c) etched with H_3PO_4

3.3. Overcasting process results

The mold was designed with a vertical parting plane, a naturally pressurized gating system, three cavities and atmospheric sprues (Fig. 8). Positioning of the foamed cores was provided by designed protrusions integrated into the milled shape of the mold.

The goal of the overcasting process was to obtain a hybrid casting with a foam core bonded to the surface with a 5 mm thick solid wall of the casting. 4 molds were made, one for each core surface modification. B1, B5 and B7 foamed cores were inserted into each of these molds. In this way, a matrix of 12 unique hybrid

castings were obtained. Four variants were determined for macroscopic and microscopic observation: hybrid casting with a non-etched B5 core, B1 core etched with HF, B7 core etched with H_3PO_4 for 1:30 min and B1 core etched with H_3PO_4 for 4 minutes (Figure 9).

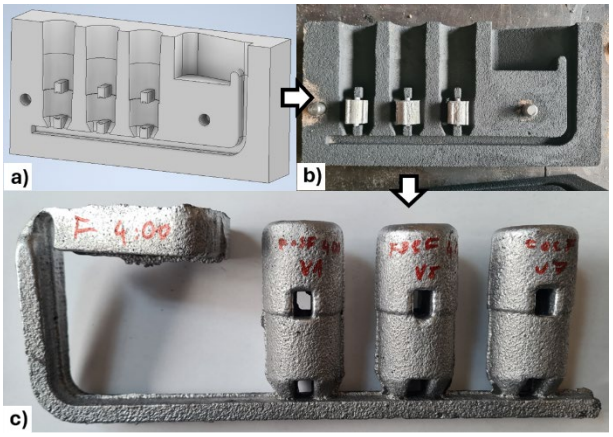

Fig. 8. Process of overcasting: a) CAD model, b) mold with fixed foam cores, c) three samples of hybrid casting

Macroscopic observation of these four samples revealed an undesirable penetration of the molten Al alloy into the pore volume of the foamed core almost to the full extent of the casting with an unetched core (Figure 9a). In the image of the HF-etched core variant (Fig. 9b), the penetration of the melt can be seen from the bottom. The distribution of the penetrated metal indicates that the melt flow disturbed the surface of the core as it entered the mold cavity. A different coloration of the core structure and melt was observed in both variants. Predicted core/casting interfaces are indicated by orange lines. The best potting result seems to be the variant etched with phosphoric acid for 1:30 min (Fig. 9c), where there was no unwanted penetration of the core by the melt.

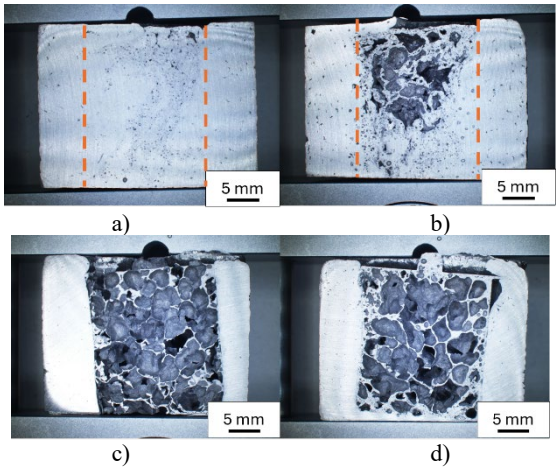

Fig. 9. Macroscopic evaluation of the hybrid castings: a) non-etched B5 core, b) B1 core etched with HF, c) B7 core etched with H_3PO_4 for 1:30 min, d) B1 core etched with H_3PO_4 for 4 minutes

3.2. EDX analysis

Cross sections of two samples were selected for EDX analysis - a hybrid casting with a core etched with HF and etched with H_3PO_4 for 1:30 min. The goal was to compare the nature and chemical composition of the resulting interfaces between the casting and the foamed core.

The sample with the HF acid-etched core was cut transversely at about half the height near the roll axis, since the interface between the casting and the porous structure can only be observed at this depth. The structure of each component is similar, with eutectic silicon present in both in the morphology of plates appearing as needles. The presence of Fe intermetallic phases can be observed (Fig. 10a). Due to the unexpected location of the interface, the presence of fluorine is negligible. It is assumed that the wall of the core was disturbed by the flow of the melt and that the observed interface was formed naturally by the solidification of the melt during its cooling, while the material of the pore walls offered some resistance to it.

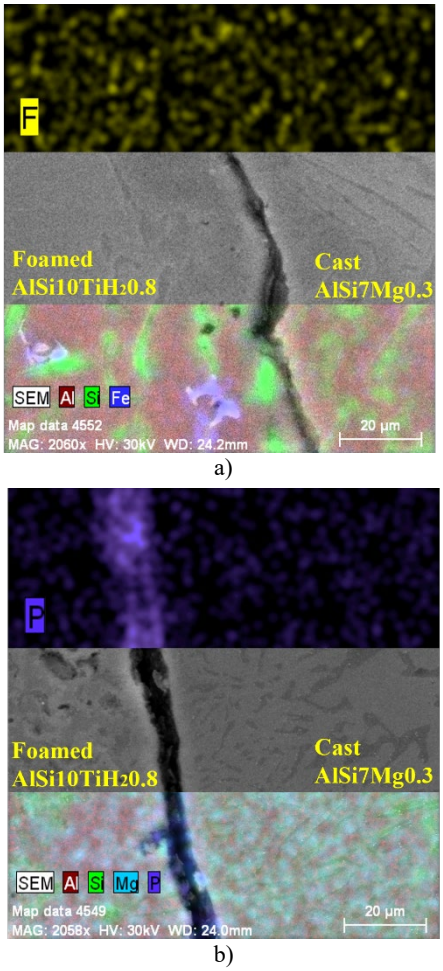

Fig. 10. EDX analysis of select hybrid castings: a) B1 core etched with HF, b) B7 core etched with H_3PO_4 for 1:30 min

On the section of the sample in which the H_3PO_4-etched core was placed, it was possible to clearly observe the outline of the foamed core, and it was possible to assume that the presence of $AlPO_4$ would be observed at this interface as a product of the reaction that took place during the surface treatment (Fig. 10b). Compared to the HF sample, the surface layer of the core was more fractured due to etching. Increasing the thickness of the interface - the gap between the cast metal and the surface of the core compared to the first sample - may seem problematic. The presence of phosphorus can be observed in this interface. It is assumed that the resulting $AlPO_4$ layer was removed during acid etching by H_2SO_4 for observation purposes for SEM and EDX analysis.

A linear EDX analysis for the presence of Si, P and O elements was performed at another point of the sample cross section with the H_3PO_4 etchant used (Fig. 11). It was observed that silicon was excluded near the interface and the concentration of P and O elements was increased. It is assumed that this is diffusion bonded $AlPO_4$ with a metal matrix, since the peak of these elements is also present on the surface of the cast metal, not only on the surface etched core.

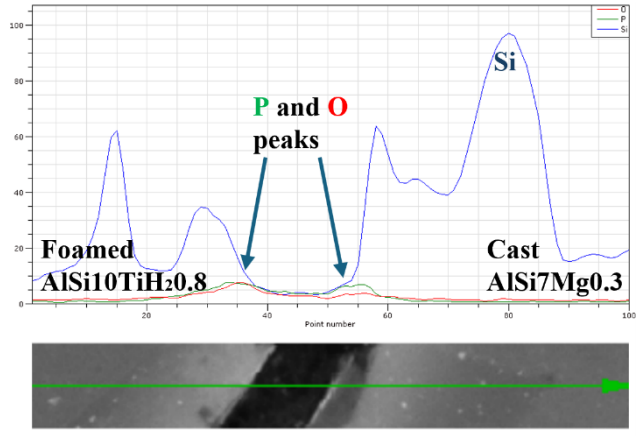

Fig. 11. Linear EDX analysis of the interface core/casting, H_3PO_4 for 1:30 min

In addition to these peaks, the presence of eutectic silicon in the form of needles can be observed in both the core matrix and the casting.

4. Conclusions

The work focused on evaluating the influence of the atmospheric pressure acting during the foaming of the material on the resulting porosity and relative density of the foamed material. A wide range of foaming pressures was deliberately used for produced samples. Based on the results obtained, it can be concluded that:

- The least suitable foaming pressure was the starting pressure of 0.2 MPa, which produced the largest pores in the board samples and the widest range of their sizes.
- The smallest variability of the results of the relative density of the molded specimens was obtained with the core variants B6 and B7, i.e. when using a starting/stabilizing pressure of 0.1 - 0.2 MPa / atm. pressure and 0.1 - 0.3 / 0.15 MPa, respectively.
- From the results of the experimental casting, it seems necessary to use a surface treatment to prevent the liquid metal from penetrating into the depth of the pores of the foamed core. The best result in this respect was obtained by surface treatment with H_3PO_4.
- Diffusion-free interfaces between the core and the casting of both observed samples were observed by EDX analysis. The presence of $AlPO_4$ as a reaction product during the surface treatment was confirmed and its additional removal during the grinding and etching of the sample for the purpose of SEM observation is assumed.

Acknowledgements

The research was created within the projects: VEGA 1/0241/23, KEGA 029ŽU-4/2023, UNIZA I-23-028-16. The authors thank for the support.

References

[1] Liu, W., Peng, T., Kishita, Y., Umeda, Y., Tang, R., Tang, W. & Hu, L. (2021). Critical life cycle inventory for aluminum die casting: A lightweight-vehicle manufacturing enabling technology. *Applied Energy.* 304, 117814. DOI: 10.1016/j.apenergy.2021.117814.

[2] Wang, B., Zhang, Z., Xu, G., Zeng, X., Hu, W. & Matsubae, K. (2023). Wrought and cast aluminum flows in China in the context of electric vehicle diffusion and automotive lightweighting. *Resources, Conservation and Recycling.* 191, 1-10, 106877. DOI: 10.1016/j.resconrec.2023.106877.

[3] Matejka, M., Bolibruchová, D. & Podprocká, R. (2021). The influence of returnable material on internal homogeneity of the high-pressure die-cast AlSi9Cu3(Fe) alloy. *Metals.* 11(7), 1-14, 1084. DOI: 10.3390/met11071084.

[4] Huang, Y., Tian, X., Li, W., He, S., Zhao, P., Hu, H., Jia, Q. & Luo, M. (2024). 3D printing of topologically optimized wing spar with continuous carbon fiber reinforced composites. *Composites Part B: Engineering.* 272, 1-9, 111166. DOI: 10.1016/j.compositesb.2023.111166

[5] Jasoliya, D., Shah, D.B., & Lakdawala, A.M. (2022). Topological optimization of wheel assembly components for all terrain vehicles. *Materials Today: Proceedings.* 59(1), 878-883. DOI: 10.1016/j.matpr.2022.01.221.

[6] Ali, M. A., Jahanzaib, M., Wasim, A., Hussain, S. & Anjum, N. A. (2018). Evaluating the effects of as-casted and aged overcasting of Al-Al joints. *The International Journal of Advanced Manufacturing Technology.* 96(1-4), 1377-1392. DOI: 10.1007/s00170-018-1682-x.

[7] Papis, K., Hallstedt, B., Löffler, J. & Uggowitzer, P. (2008). Interface formation in aluminium–aluminium compound casting. *Acta Materialia.* 56(13), 3036-3043. DOI: 10.1016/j.actamat.2008.02.042.

[8] Lefebvre, L.-P., Banhart, J. & Dunand, D.C. (2008). Porous metals and metallic foams: Current status and recent

developments. *Advanced Engineering Materials.* 10(9), 775-787. https://doi.org/10.1002/adem.200800241.
[9] Nosko, M. (2009). *Reproducibility of Aluminium Foam Properties.* Doctoral dissertation, Slovak Academy of Sciences, Bratislava, Slovak Republic.
[10] Zhang, H., Chen, Y. & Luo, A.A. (2014). A novel aluminum surface treatment for improved bonding in magnesium/aluminum bimetallic castings. *Scripta Materialia*, 86, 52-55. DOI: 10.1016/j.scriptamat.2014.05.007
[11] Rajak, D.K. & Gupta, M. (2020). *An Insight Into Metal Based Foams*. Singapore: Springer Nature. DOI: 10.1007/978-981-15-9069-6.